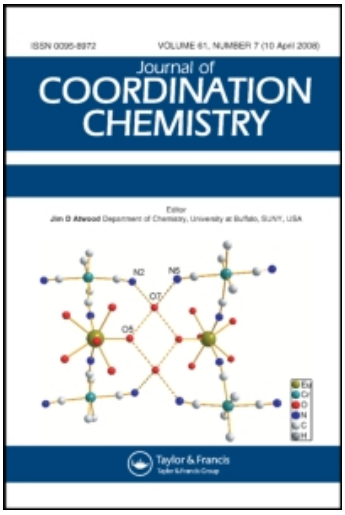

Journal of Coordination Chemistry
Publication details, including instructions for authors and subscription information:
http://www.informaworld.com/smpp/title~content=t713455674

Template synthesis and structural characterization of new diorganotin(IV) tetraazamacrocyclic complexes: precursors to produce pure phase nanosized SnO_2

Mala Nath[a]; Pramendra K. Saini[a]; George Eng[b]; Xueqing Song[b]
[a] Department of Chemistry, Indian Institute of Technology Roorkee, Roorkee 247667, Uttarakhand, India [b] Department of Chemistry and Physics, University of the District of Columbia, Washington, DC 20008, USA

First published on: 10 December 2009

To cite this Article Nath, Mala , Saini, Pramendra K. , Eng, George and Song, Xueqing(2009) 'Template synthesis and structural characterization of new diorganotin(IV) tetraazamacrocyclic complexes: precursors to produce pure phase nanosized SnO_2', Journal of Coordination Chemistry, 62: 22, 3629 — 3641, First published on: 10 December 2009 (iFirst)
To link to this Article: DOI: 10.1080/00958970903134274
URL: http://dx.doi.org/10.1080/00958970903134274

Journal of Coordination Chemistry
Vol. 62, No. 22, 20 November 2009, 3629–3641

Taylor & Francis
Taylor & Francis Group

Template synthesis and structural characterization of new diorganotin(IV) tetraazamacrocyclic complexes: precursors to produce pure phase nanosized SnO_2

MALA NATH*†, PRAMENDRA K. SAINI†, GEORGE ENG‡ and XUEQING SONG‡

†Department of Chemistry, Indian Institute of Technology Roorkee, Roorkee 247667, Uttarakhand, India
‡Department of Chemistry and Physics, University of the District of Columbia, Washington, DC 20008, USA

(*Received 3 February 2009; in final form 4 May 2009*)

This article describes the synthesis and characterization of several new diorganotin(IV) tetraazamacrocyclic complexes. The template condensation of anthranilic acid and diethylenetriamine with 1,2-dibromoethane or 1,3-dibromopropane in the presence of diorganotin(IV) dichlorides yielded macrocyclic complexes. The geometry and the mode of bonding of the resulting complexes were inferred from elemental analysis, UV-Vis, IR, Direct Analysis in Real Time-mass, (^{1}H, ^{13}C and ^{119}Sn) NMR, and ^{119m}Sn Mössbauer spectral studies. These studies suggested that the macrocyclic ligands are tetradentate, coordinating through four nitrogens giving a skew-trapezoidal bipyramidal environment around tin in the [R_2Sn(L-1)/(L-2)] (R = Me, *n*-Bu and Ph; H_2L-1/H_2L-2 = macrocyclic ligands) complexes. Thermal studies of the complexes were carried out in the temperature range 25–1000°C using thermogravimetry, derivative thermogravimetry, and differential thermal analysis techniques which provided a simple route to nanosized semi conducting SnO_2 grains, identified by X-ray diffraction analysis. The particle size of the residue, obtained by pyrolysis of **2**, **3**, **4** and **5**, determined by X-ray line broadening and transmission electron microscope were in the range ~38–48 nm and ~3–20 nm, respectively. The surface morphology of these residues was determined by scanning electron microscopy.

Keywords: Diorganotin(IV) complexes; Macrocycles; Direct Analysis in Real Time-mass (DART-mass); Pyrolysis; Nanosized SnO_2

1. Introduction

Synthetic macrocyclic compounds represent an important area of research due to their presence in many biologically significant, naturally occurring metal complexes such as metalloproteins, vitamin B_{12}, chlorophyll, etc., [1, 2]. In these macrocyclic complexes, both the metal ion and the size of ring play an important role. A number of studies have focused on physiological compatibility of azamacrocyclic compounds and the elaboration of substituents that confer biomimetic or biomedically useful properties [3].

*Corresponding author. Email: malanfcy@iitr.ernet.in

Journal of Coordination Chemistry
ISSN 0095-8972 print/ISSN 1029-0389 online
DOI: 10.1080/00958970903134274

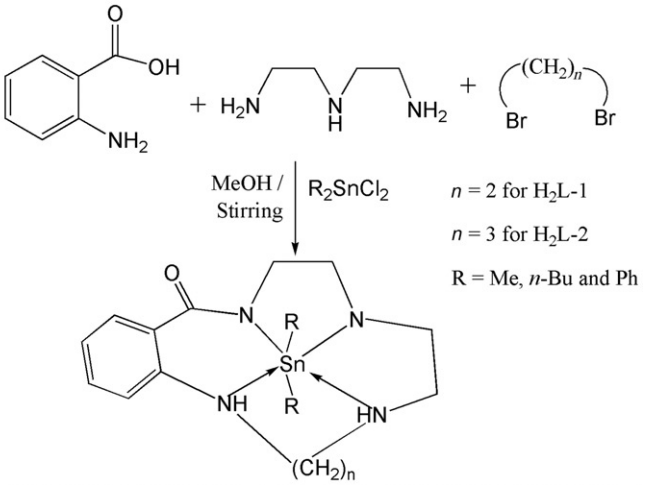

Scheme 1. Reaction pathway for diorganotin(IV) complexes of oxo-tetraazamacrocyclic ligands.

Furthermore, azamacrocycles (such as cyclam) also show antiviral activity and inhibit human immunodeficiency virus (HIV) replication [5] at least *in vitro*, and their interaction with specific peptide and DNA sequences offer interesting therapeutic possibilities [3]. They are also used as catalysts, particularly for peroxidation reactions and for electrochemical CO_2 fixation [3]. Macrocycles containing amine-amides/cyclic peptides have many properties analogous to linear peptides, and their metal complexes show resemblance to metalloproteins in function, thereby making them of biomedical interest [6]. Polyamide macrocycles are of particular interest in view of two potential donors, i.e., amide nitrogen and amide oxygen. However, in most polyamide macrocyclic complexes, amide nitrogen is involved in coordination instead of oxygen [7–10]. A large number of transition metal complexes of oxo-tetraazamacrocycles have been reported [7–14]; however, only a few reports [15–17] along with our recent report [18] are available for tin(II) and tin(IV).

Considerable attention has been paid to nanocrystalline materials due to their nanosize-dependant (2–100 nm) useful and remarkable properties [19, 20], leading to new science as well as new technologies [21, 22]. Nanoscale SnO_2 has attracted attention because of its semiconducting (an n-type with a wide band gap $E_{gap} = 3.6$ eV at 300 K), optical and electronic properties. In addition to these, SnO_2 has extensive applications such as catalytic support [23, 24], transparent conducting electrode [25] and gas sensor [26, 27].

Introductory work, reported recently by us, accounted for preparation of nanocrystalline pure-phase SnO_2 through pyrolysis of diorganotin(IV) macrocyclic complexes [18] and organotin(IV) triazolates/thiadiazolates [28–30] as single source precursors. Due to the technological applications of SnO_2, it is worth investigating the influence of ligand structure on thermal stability of organotin(IV) complexes, and to explore the best precursors for preparing such material.

Herein, we report the synthesis and characterization of several new diorganotin(IV) complexes of oxo-tetraazamacrocyclic ligands (scheme 1), obtained by template reaction of *o*-aminobenzoic acid, diethylenetetramine and 1,2-dibromoethane or

1,3-dibromopropane. Thermal decomposition of the synthesized diorganotin(IV) complexes using thermogravimetry (TGA/TG) and differential thermal analysis (DTA) techniques under air provides a simple route to SnO_2 semiconducting nanoparticles, which have been characterized by infrared (IR), X-ray diffraction analysis (XRD), scanning electron microscopy (SEM), Field Emission Scanning Electron Microscope-Energy Dispersive X-Ray (FESEM-EDX), and transmission electron microscopy (TEM) with electron diffraction analysis (TEM-ED).

2. Experimental

2.1. *Materials*

All syntheses were carried out under an anhydrous nitrogen atmosphere and precautions to avoid the presence of oxygen were taken at every stage. Dimethyltin(IV) dichloride and *n*-dibutyltin(IV) dichloride were purchased from Merk-Schuchardt and used as received. Diphenyltin(IV) dichloride was synthesized according to the reported method [31]. Anthranilic acid (Aldrich), diethylenetriamine (Koch-Light Lab.) 1,2-dibromoethane (S D Fine Chem Limited), and 1,3-dibromopropane (Aldrich) were used as received. Solvents such as methanol and cyclohexane (Qualigens) were dried and distilled, and stored under nitrogen before use.

2.2. *Measurements*

All physico-chemical and spectral measurements were carried out using similar methods and instruments reported previously [18, 28, 32], except ^{1}H, ^{13}C NMR, and ^{119}Sn NMR spectra were recorded on a Bruker Avance (500 MHz) FT NMR spectrometer using DMSO-d_6 or CD_3OD as solvent, and TMS and tetraphenyltin as the internal reference, respectively, at the Indian Institute of Technology Roorkee, Roorkee, India. The residue were prepared by the thermal decomposition of organotin(IV) precursors in a tube furnace under similar experimental conditions up to the formation temperature of SnO_2 as reported previously [18, 28–30]. The formation temperature of SnO_2 was determined by TGA.

2.3. *Synthesis*

2.3.1. Synthesis of diorganotin(IV) complexes [R_2Sn(L-1), where R = Me (1), *n*-Bu (2) and Ph (3)] of 3-oxo-1,2-benzo-4,7,10,13-tetraazacyclotridecane (H_2L-1). Dimethyltin(IV), dibutyltin(IV) and diphenyltin(IV) complexes of H_2L-1 were prepared by dropwise addition of methanol solution (~10 mL) for each of diethylenetriamine (0.155 g, 1.5 mmol) and *o*-aminobenzoic acid (0.206 g, 1.5 mmol) to the solution of dimethyltin(IV) dichloride (0.299 g, 1.5 mmol), dibutyltin(IV) dichloride (0.456 g, 1.5 mmol), or diphenyltin(IV) dichloride (0.516 g, 1.5 mmol) in dry methanol (~10 mL) in a two-neck flask with constant stirring at room temperature under dry nitrogen. The resultant mixture was stirred for 7 h at room temperature, and then the methanol solution of 1,2-dibromoethane (0.282 g, 1.5 mmol) was added dropwise.

The stirring was continued for another 5 h at room temperature, resulting in formation of the title compounds. Excess solvent was reduced under vacuum and solid product was washed thoroughly by dry cyclohexane, and then dried *in vacuo*.

Me_2Sn(L-1) (**1**): Brown solid; m.p., 170–172°C; Yield, 0.58 g (62%); Anal. Calcd for $C_{15}H_{24}N_4OSn$ (%) (395.09): C, 45.60; H, 6.12; N, 14.18; Sn, 30.05. Found: C, 45.36; H, 6.01; N, 13.79; Sn, 29.72. (MH^+/z) Found (Calcd): 396.08 (396.10); UV-Vis [THF, λ_{max}(nm) ($\varepsilon(M^{-1}cm^{-1})$)]: 266 (4148), 337 (16470); Selected IR data (KBr, $\nu_{max}(cm^{-1})$): 1619vs (νC=O)/amide I, 1578m (ν C–N + δNH)/amide II, 1255vs (δN–H)/amide III, 667m (ϕC=O), 612w (ν_{as} Sn–C), 564m (ν_s Sn–C), 439m (ν Sn–N), 420m (ν Sn←N); ^{119m}Sn Mössbauer: Q.S. = 2.068 mm s^{-1}, I.S. = 0.816 mm s^{-1}, ρ(Q.S./I.S.) = 2.53, τ_1(L) = 1.884, τ_2(R) = 2.086, ∠C–Sn–C = 99.76°.

n-Bu_2Sn(L-1) (**2**): Cream solid; m.p., 123–125°C; Yield, 0.96 g (87%); Anal. Calcd for $C_{21}H_{36}N_4OSn$ (%) (479.25): C, 52.63; H, 7.57; N, 11.69; Sn, 24.77. Found: C, 52.26; H, 7.11; N, 11.39; Sn, 24.64. (MH^+/z) Found (Calcd): 480.29 (480.26); UV-Vis [THF, λ_{max}(nm) ($\varepsilon(M^{-1}cm^{-1})$)]: 265 (4834), 338 (23584); Selected IR data (KBr, ν_{max}/cm^{-1}): 1619vs (νC=O)/amide I, 1576m (ν C–N + δNH)/amide II, 1254vs (δN–H)/amide III, 666m (ϕC=O), 639m (ν_{as} Sn–C), 564w (ν_s Sn–C), 441m (ν Sn–N), 406m (ν Sn←N); ^{119m}Sn Mössbauer: Q.S. = 2.109 mm s^{-1}, I.S. = 0.890 mm s^{-1}, ρ(Q.S./I.S.) = 2.37, τ_1(L) = 1.704, τ_2(R) = 1.905, ∠C–Sn–C = 97.28°.

Ph_2Sn(L-1) (**3**): Cream solid; m.p., 168–170°C; Yield, 0.93 g (80%); Anal. Calcd for $C_{25}H_{28}N_4OSn$ (%) (519.23): C, 57.83; H, 5.44; N, 10.79; Sn, 22.86. Found: C, 57.64; H, 5.32; N, 10.15; Sn, 21.95. (MH^+/z) Found (Calcd): 520.25 (520.24); UV-Vis [THF, λ_{max}(nm) ($\varepsilon(M^{-1}cm^{-1})$)]: 265 (4988), 339 (22192); Selected IR data (KBr, ν_{max}/cm^{-1}): 1619m (νC=O)/amide I, 1576vs (ν C–N + δNH)/amide II, 1257vs (δN–H)/amide III, 666w (ϕC=O), 248s (ν_{as} Sn–C), 224m (ν_s Sn–C), 445w (ν Sn–N), 426w (ν Sn←N).

2.3.2. Synthesis of diorganotin(IV) complexes [R_2Sn(L-2), where R = Me (4), *n*-Bu (5) and Ph (6)] of 3-oxo-1,2-benzo-4,7,10,14-tetraazacyclotetradecane (H_2L-2). The procedure used for these complexes was similar to the method mentioned in 2.3.1, except 1,3-dibromopropane (0.303 g, 1.5 mmol) was added instead of 1,2-dibromoethane in the final step.

Me_2Sn(L-2) (**4**): Brown solid; m.p., 156–158°C; Yield, 0.77 g (80%); Anal. Calcd for $C_{16}H_{26}N_4OSn$ (%) (409.12): C, 46.97; H, 6.41; N, 13.70; Sn, 29.07. Found: C, 46.89; H, 6.16; N, 13.46; Sn, 28.69. (MH^+/z) Found (Calcd): 410.15 (410.13); UV-Vis [THF, λ_{max}(nm) ($\varepsilon(M^{-1}cm^{-1})$)]: 266 (7674), 337 (27126); Selected IR data (KBr, ν_{max}/cm^{-1}): 1619s (νC=O)/amide I, 1579s (ν C–N + δNH)/amide II, 1256vs (δN–H)/amide III, 666m (ϕC=O), 649s (ν_{as} Sn–C), 527w (ν_s Sn–C), 469m (ν Sn–N), 420m (ν Sn ← N).

n-Bu_2Sn(L-2) (**5**): Cream solid; m.p., 115–117°C; Yield, 0.91 g (81%); Anal. Calcd for $C_{22}H_{38}N_4OSn$ (%) (493.28): C, 53.57; H, 7.76; N, 11.36; Sn, 24.07. Found: C, 52.85; H, 7.22; N, 11.07; Sn, 23.93. (MH^+/z) Found (Calcd): 494.29 (494.29); UV-Vis [THF, λ_{max}/nm ($\varepsilon/M^{-1}cm^{-1}$)]: 265 (7830), 338 (26538); Selected IR data (KBr, ν_{max}/cm^{-1}): 1620s (νC=O)/amide I, 1577w (ν C–N + δNH)/amide II, 1255vs (δN–H)/amide III, 666m (ϕC=O), 637s (ν_{as} Sn–C), 561w (ν_s Sn–C), 440w (ν Sn–N), 421m (ν Sn←N).

Ph_2Sn(L-2) (**6**): Cream solid; m.p., 188–190°C; Yield, 0.72 g (61%); Anal. Calcd for $C_{26}H_{30}N_4OSn$ (%) (533.26): C, 58.56; H, 5.67; N, 10.51; Sn, 22.26. Found: C, 57.92; H, 5.18; N, 10.65; Sn, 21.84. (MH^+/z) Found (Calcd): 534.27 (534.27); UV-Vis [THF,

λ_{max}(nm) (ε($M^{-1}cm^{-1}$))]: 266 (8146), 341 (15800); Selected IR data (KBr, ν_{max}/cm^{-1}): 1618s (νC=O)/amide I, 1579m (ν C−N + δNH)/amide II, 1257s (δN−H)/amide III, 665m (ϕC=O), 279m (ν_{as} Sn−C), 227vs (ν_s Sn−C), 449w (ν Sn−N), 416w (ν Sn←N); ^{119m}Sn Mössbauer: Q.S. = 1.869 mm s^{-1}, I.S. = 0.860 mm s^{-1}, ρ(Q.S./I.S.) = 2.17, τ_1(L) = 1.880, τ_2(R) = 1.991, ∠C–Sn–C = 90.00°.

Note: vs: very strong; s: strong; m: medium; w: weak; Q.S.: quadrupole splitting; I.S.: isomer shift; τ_1(L): half line width left doublet component; τ_2(R): half line width right doublet component.

3. Results and discussion

The reactions involved (scheme 1) in the synthesis of diorganotin(IV) complexes of H_2L-1 and H_2L-2 were quite feasible and required 14 h of stirring at ambient temperature (30 ± 2°C). All the synthesized complexes are cream to brown solids, stable towards air and moisture, and sparingly soluble in methanol and dimethylsulphoxide but exhibit very poor solubility in other organic solvents. The elemental analyses and the molecular ion peaks observed in the Direct Analysis in Real Time (DART)-mass spectra of diorganotin(IV) complexes of H_2L-1 or H_2L-2 support formation of the macrocyclic ligand framework (scheme 1). The molar conductances in methanol (10^{-3} M) lie in the range 10.0–60.0 $Ohm^{-1}cm^2mol^{-1}$, indicating non-electrolytes. Despite many attempts, good crystals for X-ray crystallography could not be obtained.

3.1. *Electronic spectral studies in solution*

The electronic spectral bands (in nm) together with their ε (molar extinction coefficient) values of the diorganotin(IV) complexes are presented in the experimental section. The spectra exhibit two absorption bands at 265 ± 1 and 339 ± 2 nm, which may be assigned to $n \rightarrow \pi^*$ transitions of the chromophore (>C=O) and ligand to metal charge transfer/1B band of phenyl ring, respectively.

3.2. *IR spectral studies*

The most significant bands of diorganotin(IV) complexes of macroyclic ligands recorded in IR region have been presented in the experimental section. The preliminary identification of the synthesized diorganotin(IV) complexes of macrocyclic ligands have been obtained from their IR spectra which show the absence of uncondensed functional groups (NH_2, O−H), stretching modes of starting materials and the appearance of bands characteristic of secondary amine and amide groups. Four amide bands have been identified in the IR spectra of complexes studied herein at 1619 ± 1, 1578 ± 2, 1256 ± 2 and 666 ± 1 cm^{-1} assignable to amide-I ν(C=O); amide II (νC−N + δNH); amide III δ(N−H) and amide IV ϕ(C=O), respectively, suggesting formation of the proposed macrocyclic framework similar to that reported for metal complexes of other tetraazamacrocyclic ligands [14, 18]. The absence of ν(Sn−O) rules out involvement

of C=O in coordination. Further, appearance of low intensity bands in the region 470–406 cm^{-1}, assignable to ν(Sn−N)/(Sn←N) vibrational modes in the spectra of diorganotin(IV) complexes, confirm coordination of all four nitrogens to tin [18]. The ν_{as}(Sn−C) and ν(Sn−C) in all dialkyltin(IV) complexes have been observed at 631 ± 19 and $546 \pm 19\,cm^{-1}$, respectively, whereas corresponding vibrational bands in diphenyltin(IV) analogues are observed in far-IR region at 264 ± 16 and $226 \pm 2\,cm^{-1}$, respectively [33].

3.3. *DART-mass spectral studies*

The mass spectra of complexes **1**–**6** have been recorded in the solid state by a recently developed technique (DART)-mass spectrometer. The molecular ion peaks (due to ^{119}Sn isotope) in all the synthesized complexes have been observed at *m*/*z* 396.08, 480.29, 520.25, 410.15, 494.29, and 534.27, suggesting the proposed molecular formula of (**1**), (**2**), (**3**), (**4**), (**5**), and (**6**), respectively, and supporting the monomeric nature of all the synthesized complexes. The peaks at M + 1, M − 1 and M − 2 have also been observed due to the presence of ^{120}Sn, ^{118}Sn, and ^{117}Sn isotopes [34], respectively.

In **1**–**3** and **4**–**5** peaks have been observed at *m*/*z* 247.38 ± 0.01 and 261.37 ± 0.02, respectively, indicating the fragmentation of complexes and corresponding to the LH^+ (deprotonated corresponding macrocycles). Other significant peaks are listed in table 1. The ion peaks observed in **1**–**6** at *m*/*z* 126, 120, 114, 104 and 87 correspond to $[C_6H_{10}N_2O]^+$, $[SnH]^+$, $[C_5H_{12}N_3]^+$, $[C_7H_4O]^+$, and $[C_4H_{11}N_2]^+$, respectively, indicating further fragmentation of the species. In **4**–**6** two more peaks are observed at *m*/*z* 138 and 61, due to $[C_7H_{10}N_2O]^+$ and $[C_3H_{10}N]^+/[C_2H_7NO]^+$ [18], respectively. The mass spectral data help to establish the structure along with the corresponding macrocyclic framework and is informative about purity and molecular weight of the synthesized complexes.

3.4. *^{119m}Sn Mössbauer spectral studies*

The ^{119m}Sn Mössbauer spectra of Me_2Sn(L-1), *n*-Bu_2Sn(L-1) and Ph_2Sn(L-2) were recorded at 80 K (spectral data presented in the experimental section). Mössbauer spectra exhibit a doublet centered in the I.S. range 0.816–0.890 mm s^{-1} and Q.S.

Table 1. DART-mass spectral data of the diorganotin(IV) complexes of H_2L-1[a] and H_2L-2[b].

Compound	(MH^+/z)[c]	(LH^+/z)[d]	Other peaks[e]
1	396.08	247.38	126, 120, 114, 104, 87
2	480.29	247.38	126, 120, 114, 104, 87
3	520.25	247.39	126, 120, 114, 104, 87
4	410.15	261.38	138, 120, 104, 87, 61,
5	494.29	261.35	138, 126, 120, 114, 104, 87, 61
6	534.27	261.35	138, 126, 120, 114, 104, 87, 61

[a]$C_{13}H_{20}N_4O$ (248.33); [b]$C_{14}H_{22}N_4O$ (262.36); [c]molecular ion peaks of complexes; [d]corresponding deprotonated macrocyclic ligand peak; [e]molecular ion peaks for various fragments as presented in corresponding section.

values in the range 1.869–2.109 mm s^{-1}, showing that the electric field gradient around tin is generated by inequalities in tin–nitrogen (ligand) σ bond and is also due to geometric distortions. The low value of Q.S. for Ph_2Sn(L-2) is due to greater polarizability of the phenyl groups. The ρ (Q.S./I.S.) value of greater than 2 indicates coordination number of tin either 5 or 6 [35] in the studied diorganotin(IV) complexes.

The Q.S. values for *trans*- and *cis*-octahedral $[R_2SnX_4]^{2-}$ are around 4.00 and 2.00 mm s^{-1}, respectively [36]. Further, it has been reported [36] that I.S. values for *cis*-$[R_2SnX_4]^{2-}$ are less than 1.00 mm s^{-1} while those for *trans*-$[R_2SnX_4]^{2-}$ are approximately 1.2–1.3 mm s^{-1}. The observed values of Q.S. and I.S. of the studied diorganotin(IV) complexes of macrocyclic ligands are substantially lower than the values for *trans*-octahedral configuration and correspond to values for *cis*-octahedral configuration. Further, the ∠C–Sn–C for the studied diorganotin(IV) complexes has been calculated using Parish's relationship [37]: $Q.S. = 4[R][1-3/4\sin^2 2\theta]^{1/2}$, where ∠C–Sn–C is $(180-2\theta)^\circ$ and [R] is the partial quadruple splitting for alkyl and phenyl groups bonded to tin. The reported values of [R] for alkyl and phenyl groups are -1.03 mm s^{-1} and -0.95 mm s^{-1}, respectively [38, 39]. The calculated values of ∠C–Sn–C in the studied diorganotin(IV) complexes of macrocyclic ligands are in the range of 90–100°, which correspond to *cis*-octahedral geometry with distortion due to steric strain of the ligand. The structures of R_2Sn(L-1) and R_2Sn(L-2) are best described as highly distorted square bipyramidal/skew-trapezoidal bipyramidal configuration with the two organic groups (Me, *n*-Bu or Ph) in bent axial position and the trapezoidal plane defined by the four Sn–N coordination/interactions and macrocyclic ligand is in saddle conformation (figures 1 and 2). The observed ν_{as}(Sn–C) and ν_s(Sn–C) stretching vibrations in the IR spectra of the studied diorganotin(IV) complexes also indicated a non-linear SnC_2 fragment (*cis*-organic groups) and ruled out the possibility of *trans*-octahedral structure.

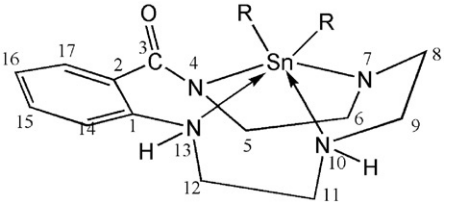

Figure 1. Proposed structure of diorganotin(IV) complexes of H_2L-1, where R = Me, *n*-Bu or Ph.

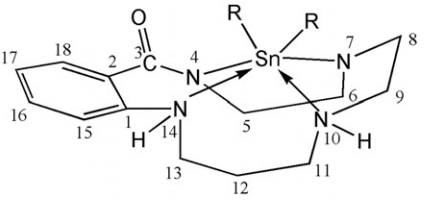

Figure 2. Proposed structure of diorganotin(IV) complexes of H_2L-2, where R = Me, *n*-Bu or Ph.

3.5. *^{1}H, ^{13}C, and ^{119}Sn NMR solution spectral studies*

^{1}H, ^{13}C, and ^{119}Sn NMR chemical shifts along with coupling constants obtained from solutions of **1**–**6** are summarized in Supplemental Material. The ^{1}H NMR spectra of the complexes do not show any signal assignable to carboxylic and primary amino protons supporting the proposed macrocyclic skeleton in scheme 1. The complexes showed doublet and multiplets in the region δ 6.63−8.10 ppm corresponding to phenyl ring protons. Multiplets observed for all the complexes in the regions δ 3.03−3.35 and 2.45−2.94 ppm may be assigned to methylene protons between the nitrogens (–CH_2–N) [13]. The signals for NH could not be located in the δ 0−15 ppm region in all of the complexes. Characteristic signals for alkyl- and aryl-hydrogens of organotin(IV) moieties are in good agreement with reported values [32]. The $^{2}J(^{1}H-^{119}Sn)$ values calculated for complexes **1**, **2**, **4** and **5** are 99.44, 98.99, 98.24, and 99.41 Hz, respectively, in the range for six-coordinate diorganotin(IV) complexes.

In ^{13}C NMR spectra of complexes, a resonance in the region δ 169.74−176.65 ppm has been assigned to amide (−NH−C=O) carbon. All the magnetically non-equivalent carbons of aryl and alkyl groups of macrocyclic framework have been assigned. All magnetically non-equivalent carbons of the alkyl or phenyl groups attached to tin have also been identified and their chemical shift values are in close agreement with reported values [32]. The $^{1}J(^{13}C-^{119}Sn)$ values have been calculated for **1**–**6** from their ^{13}C NMR spectra. But the ^{117}Sn and ^{119}Sn satellites are not well-resolved in spectra, so $^{1}J(^{13}C-^{119}Sn)$ was calculated from the distance separating the center of fused ^{117}Sn and ^{119}Sn satellites × 1.023 (because the natural abundances of ^{117}Sn and ^{119}Sn are similar (7.6% and 8.6%, respectively) the differences between the separation of the centers of unresolved satellites and $^{1}J(^{13}C-^{119}Sn)$ is closely approximated by multiplying the separation, in hertz by one half the ratio of the gyromagnetic ratio of ^{119}Sn and ^{117}Sn) [40]. $^{1}J(^{13}C-^{119}Sn)$ values calculated for **1**–**6** are 699.15, 712.91, 649.75, 587.64, 651.98, and 652.94 Hz, respectively, which lie in the range for six-coordinate diorganotin(IV) complexes [41]. Moreover, the calculated values of ∠C−Sn−C using the observed $^{1}J(^{13}C-^{119}Sn)$ values in the equation given by Lockhart and Manders [42] ($|^{1}J| = 11.4(\theta) - 875$) are in the range of 128.3−139.3°, indicating a highly distorted square pyramidal or skew-trapezoidal geometry. These ∠C−Sn−C are greater than those obtained in the solid-state due to solvent effects.

The ^{119}Sn NMR chemical shifts are very sensitive to coordination number of tin and are greatly shifted up-field on bonding to Lewis base. The ^{119}Sn NMR spectra of the complexes were recorded in CD_3OD or DMSO-d_6 in order to obtain additional support for the conclusions drawn by ^{1}H and ^{13}C NMR. In the ^{119}Sn NMR spectra of **1**–**6**, the ^{119}Sn chemical shifts are observed at δ (−405.97), (−300.99), (−429.50, −472.18), (−404.81), (−231.99), and (−392.29, −401.05 and −429.50) ppm, respectively. As reported in the literature [43], values of ^{119}Sn chemical shifts in the range 200 to −60, −90 to −190 and −210 to −400 ppm have been associated with four-, five-, and six-coordinate tin centers, respectively. The observed ^{119}Sn chemical shifts of the studied compounds are in the range of six-coordinate tin compounds and show an upward shift as compared to the reactants Me_2SnCl_2 ($\delta = 137$ ppm) and *n*-Bu_2SnCl_2 ($\delta = 154$ ppm) [44]. Therefore, ^{119}Sn, ^{1}H and ^{13}C NMR spectral data reveal that the interactions between tin and four N atoms in solution (as existing in the solid-state supported by IR and ^{119m}Sn Mössbauer) lead to the skew-trapezoidal bipyramidal geometry around tin in these studied complexes.

3.6. *Thermal studies*

Thermal decomposition behavior of **1**–**6** in air has been studied using TG, derivative thermogravimetry (DTG) and DTA techniques. The TG temperature ranges, peak temperatures in DTA and DTG, percent weight loss along with the species lost as well as enthalpy of DTA peaks, are presented in table 2. The TG and DTA curves of the complexes are presented in "Supplementary material". The main diffraction lines observed in the residues (Supplementary material) obtained by the pyrolysis of these organotin(IV) macrocyclic complexes are summarized in table 3.

The TGA profiles show two overlapping decomposition steps for **1**, **2**, and **5** and three decomposition steps for **3**, **4**, and **6**. The first weight loss starts at ca 99–100°C and completes at ca 620–650°C. The total mass loss, including all steps, corresponds to the value calculated for the loss of all organic moieties. In the last step of decomposition, an exothermic peak appears at 584 ± 42°C with very high enthalpy, which may be due to the decomposition of the remaining organic moieties along with simultaneous oxidation of the material to SnO_2. The residue obtained at 550 ± 50°C is SnO_2, characterized by XRD (table 3), in which main diffraction lines were matched with reported values of SnO_2 [45]. This was further supported by the presence of only ν(Sn–O) at $622 \pm 20\,cm^{-1}$ [33] in the IR spectra. The weights of the residues at $\geq$650°C are less than the calculated value due to sublimation [28, 29]. The crystallite average size calculated by the Scherrer equation [26, 46] is in the range 38–48 nm (table 3).

The SEM images of the residues obtained by thermal decomposition of *n*-Bu_2Sn(L-1) and Me_2Sn(L-2) at 550 ± 50°C are shown in figures 3(a) and 3(b), respectively. The residues obtained by the pyrolysis of diorganotin(IV) macrocycles was agitated ultrasonically for 30 min. The SEM images of the residues showed uniform grain size with almost spherical shape. The grain size measured by SEM is in the range of ~20–200 nm in diameter. FE-SEM images of the residues obtained by pyrolysis of **2**, **3**, **4** and **5** with EDX analysis have been recorded and also depicted the formation of almost spherical particles. EDX analysis of these particles in SEM micrographs at various locations marked with the sign '+' show that they consist of Sn and O with SnO_2 composition in wt%, which are in good agreement with the calculated%.

The size of the particle of residues (SnO_2) obtained in case of Bu_2Sn(L-1), Ph_2Sn(L-1), Me_2Sn(L-2) and *n*-Bu_2Sn(L-2) measured by TEM is in the range of ~3–20 nm (figure 4 and Supplementary material). There are many grains and holes about 5–20 nm size. Many connected grains form a random network, in which various nanosized holes appear. Such structure is named a nanosponge [23]. There are a large number of nanometer grains with well-ordered lattices. The electron diffraction pattern of a selected area appeared to be typical polycrystalline diffraction rings. According to the diameters of the rings, the spacings are 0.33, 0.026, 0.024 nm for all analyzed complexes, which correspond to the spacing of [110], [101], and [200], respectively, of tetragonal SnO_2. This indicates that the grains are nanocrystalline tetragonal SnO_2 [23]. On the basis of the above studies, Ph_2Sn(L-1) is the best precursor among the studied diorganotin(IV) derivatives of macrocycles for production of nanosized SnO_2.

4. Conclusions

Diorganotin(IV) complexes of tetraazamacrocycles have been synthesized through template method. The solid-state and solution spectral studies along with elemental

Table 2. Thermal analysis data of organotin(IV) derivatives in air.

Compound	Step no.	Temp. range in TG (°C)	Peak temp. in DTG (°C)	Peak temp. in DTA (°C)	Enthalpy ($mJ\,mg^{-1}$)	Loss of mass % Observed (calculated)	Species lost
Me_2Sn(L-1) (**1**)	I	100–249	185 235	157 (endothermic) 184 (endothermic) 235 (endothermic)	464	51.47 (51.70)	$C_{11}H_{13}N_2O + CH_3$
	II	249–620	576	575 (exothermic)	−1508	18.14 (17.99)	$C_3H_8N_2$ + oxidation & sublimation
Bu_2Sn(L-1) (**2**)	I	100–270	259	157 (endothermic) 260 (endothermic)	97.3 236	69.31 (73.31)	Ligand moiety + $2(C_4H_9)$
	II	270–620	–	583 (exothermic)	−1039	22.69	Sublimation
Ph_2Sn(L-1) (**3**)	I	100–250	230	166 (endothermic)	223	47.54 (47.44)	$C_{13}H_{18}N_4O$
	II	250–431	–	266 (exothermic) 372 (exothermic) 417 (exothermic)	−140 −34.6 −42.2	28.53 (29.70)	$2C_6H_5$
	III	431–620	–	557 (broad exothermic)	−1197	13.93	Oxidation & sublimation
Me_2Sn(L-2) (**4**)	I	99–250	243	160 (endothermic) 243 (endothermic)	529	49.91 (49.68)	$C_{12}H_{15}N_2O$
	II	250–320	310	312 (endothermic)	71.6	21.00 (21.05)	$C_4H_{11}N_2$
	III	320–620	567	564 (exothermic)	−1208	23.19	Oxidation & sublimation
Bu_2Sn(L-2) (**5**)	I	99–267	261	160 (endothermic) 263 (endothermic)	85.7 96.3	74.28 (75.93)	Ligand moiety + $2(C_4H_9)$
	II	267–620	–	542 (exothermic)	−1097	21.72	Oxidation & sublimation
Ph_2SnL-2 (**6**)	I	99–250	229	162 (endothermic)	74.9	35.8 (34.17)	$C_7H_5O + C_6H_5$
	II	250–329	314	273 (exothermic)	−288	19.71 (18.78)	$C_5H_{12}N_2$
	III	329–650	435 625	387 (exothermic) 435 (exothermic) 626 (exothermic)	−184 −56.1 −1112	21.95 (24.97)	$C_2H_3N_2 + C_6H_5$

Table 3. The main diffraction lines (intensity) and crystallite average size calculated by the Scherrer equation for the residue obtained.

Tin compound/ Residue of complex	Main diffraction lines *d* (Å) (intensity (%)) (*h k l*) 1	2	3	4	5	Average size *D* (nm)
Sn[a]	2.92 (100) (2 0 0)	2.79 (90) (1 0 1)	2.06 (34) (2 2 0)	2.02 (74) (2 1 1)	1.48 (23) (1 1 2)	–
SnO[a]	3.39 (100)	3.00 (50)	2.89 (90)	2.67 (90)	1.77 (80)	–
SnO_2[a]	3.35 (100) (1 1 0)	2.64 (80) (1 0 1)	2.37 (25) (2 0 0)	1.77 (65) (2 1 1)	1.68 (18) (2 2 0)	–
n-Bu_2Sn(L-1)	3.34 (100)	2.64 (90)	2.36 (23)	1.76 (67)	1.67 (15)	47.89
Ph_2Sn(L-1)	3.34 (100)	2.64 (73)	2.36 (21)	1.76 (57)	1.67 (12)	37.79
Me_2Sn(L-2)	3.34 (100)	2.64 (92)	2.36 (24)	1.76 (89)	1.67 (20)	47.34
n-Bu_2Sn(L-2)	3.34 (100)	2.64 (84)	2.36 (22)	1.76 (70)	1.67 (17)	40.90

[a]Ref. [45].

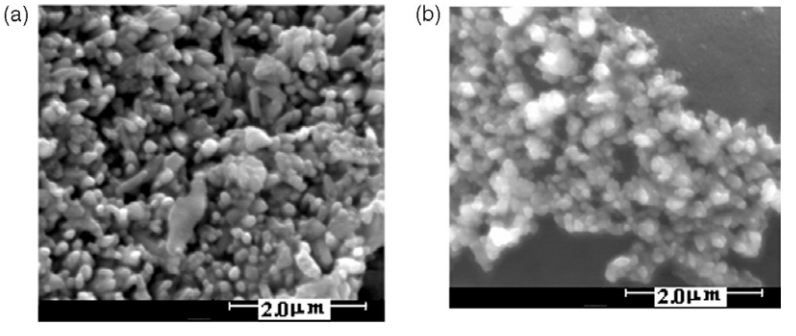

Figure 3. SEM images of residue obtained by pyrolysis of (a) *n*-Bu_2Sn(L-1) (**2**), (b) Me_2Sn(L-2) (**4**).

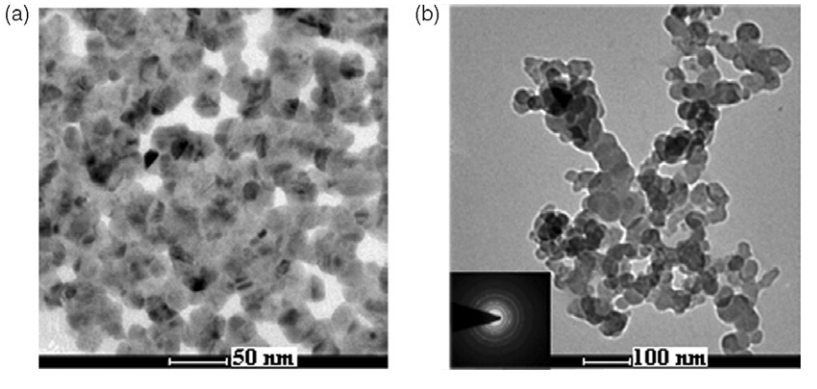

Figure 4. TEM images of residue obtained by pyrolysis of Me_2Sn(L-2) (**4**) with electron diffraction pattern.

Table 4. Comparison of average size of the residues (SnO_2), calculated by XRD, SEM, and TEM.

Residue of compounds	Grain size by XRD (nm)	Grain size by SEM (nm)	Grain size by TEM (nm)
n-Bu_2SnL-1 (**2**)	47.89	20–200	5–10
Ph_2SnL-1 (**3**)	37.79	20–100	3–10
Me_2SnL-2 (**4**)	47.34	40–150	5–15
n-Bu_2SnL-2 (**5**)	40.90	20–100	5–20

analysis of all the synthesized complexes, $R_2Sn(L\text{-}1)/R_2Sn(L\text{-}2)$, suggest a skew-trapezoidal bipyramidal environment around tin with the two organic groups in bent axial position and trapezoidal plane being defined by four Sn–N interactions. Thermal decomposition of the complexes yielded SnO_2, which is confirmed by X-ray diffraction. The crystallite average size of SnO_2 calculated by the Scherrer equation is in the range 38–48 nm, whereas the size measured by SEM and TEM are in the range of ~20–200 nm and ~3–20 nm, respectively, in diameter (table 4). Ph_2SnL-1 is the best precursor among the studied diorganotin(IV) derivatives of macrocycles for the production of nanosized SnO_2.

Acknowledgments

The authors are thankful to the Head, Institute Instrumentation Center, Indian Institute of Technology Roorkee, Roorkee, India, for providing facilities to carry out (^1H, ^{13}C, and ^{119}Sn) NMR measurements, thermal studies, X-ray diffraction analysis and SEM, FE-SEM, and TEM images, and the Head, Regional Sophisticated Instrumentation Center, the Central Drug Research Institute, Lucknow, India, for providing DART-mass spectral studies. One of the authors (P.K. Saini) is thankful to the Council of Scientific and Industrial Research, New Delhi, India, for awarding Junior Research Fellowship.

References

[1] P.V. Bernhardt, G.A. Lawrance. *Coord. Chem. Rev.*, **104**, 297 (1990).
[2] J.E. Huheey, E.A. Keiter, R.L. Keiter. *Textbook of Inorganic Chemistry*, Pearson Education, Singapore (2000).
[3] N.F. Curtis. *Comprehensive Coordination Chemistry II*, p. 447, Elsevier Pergamon, Amsterdam (2004), and references therein.
[4] C.W. Schwietert, J.P. McCue. *Coord. Chem. Rev.*, **184**, 67 (1999).
[5] T.M. Hunter, S.J. Paisey, H.S. Park, L. Cleghorn, A. Parkin, S. Parsons, P.J. Sadler. *J. Inorg. Biochem.*, **98**, 713 (2004).
[6] H. Miyake, Y. Kojima. *Coord. Chem. Rev.*, **148**, 301 (1996).
[7] M. Shakir, S.P. Varkey, P.S. Hameed. *Polyhedron*, **12**, 2775 (1993).
[8] H.A.O. Hill, K.A. Raspin. *J. Chem. Soc., Dalton Trans.*, 3036 (1968).
[9] N.W. Alcock, P. Moore, H.A.A. Omar, C.J. Reader. *J. Chem. Soc., Dalton Trans.*, 2643 (1987).
[10] M. Shakir, S.P. Varkey, T.A. Khan. *Indian J. Chem.*, **34A**, 72 (1995).
[11] M.B. Inoue, C.A. Villegas, K. Asano, M. Nakamura, M. Inoue, Q. Fernado. *Inorg. Chem.*, **31**, 2480 (1992).

[12] J.F. Carvolho, S.H. Kim, C.A. Chang. *Inorg. Chem.*, **31**, 4065 (1992).
[13] T.A. Khan, S.S. Hasan, N. Jahan, K.S. Islam. *Indian J. Chem.*, **39A**, 450 (2000).
[14] S.J. Swamy, S. Pola. *Spectrochim. Acta, Part A*, **70**, 929 (2008).
[15] P.R. Shukla, M.C. Sharma, M. Bhatt, N. Ahmad, S.K. Srivastava. *Indian J. Chem.*, **29A**, 186 (1990).
[16] A. Chaudhary, S. Dave, R. Swaroop, R.V. Singh. *J. Indian Chem. Soc.*, **79**, 371 (2002).
[17] G.R. Willey, M.D. Rudd. *Polyhedron*, **26**, 2805 (1992).
[18] M. Nath, P.K. Saini, G. Eng, X. Song. *J. Organomet. Chem.*, **693**, 2271 (2008).
[19] S.A. Majetich, J.H. Scott, E.M. Kirkpatrick, K. Chowdary, K. Gallagher, M.E. McHenry. *NanoStruct. Mater.*, **9**, 291 (1997).
[20] A.K. Menon, B.K. Gupta. *NanoStruct. Mater.*, **12**, 1117 (1999).
[21] A. Robertson, U. Erb, G. Palumbo. *NanoStruct. Mater.*, **12**, 1035 (1999).
[22] D.J. Sellmyer, M. Yu, R.D. Kirby. *NanoStruct. Mater.*, **12**, 1021 (1999).
[23] W. Dazhi, W. Shulin, C. Jun, Z. Suyuan, L. Fangqing. *Phys. Rev. B.*, **49**, 14282 (1994).
[24] D.E. Williams, K.F.E. Pratt. *J. Chem. Soc. Farad. Trans.*, **94**, 3493 (1998).
[25] T.E. Moustafid, H. Cachet, B. Tribollet, D. Festy. *Electrochim. Acta*, **47**, 1209 (2002).
[26] A.R. Phani, S. Manorama, V.J. Rao. *Mater. Chem. Phys.*, **58**, 101 (1999).
[27] G.J. Li, X.H. Zhang, S. Kawi. *Sens. Actuators, B.*, **60**, 64 (1999).
[28] M. Nath, Sulaxna. *Thermochim. Acta.*, **489**, 27 (2008).
[29] M. Nath, Sulaxna. *Mater. Res. Bull.*, **41**, 78 (2006).
[30] M. Nath, Sulaxna. *Indian J. Chem.*, **47A**, 510 (2008).
[31] R.C. Poller. *The Chemistry of Organotin Compounds*, p. 315, Logos Press, London (1970).
[32] M. Nath, S. Pokharia, G. Eng, X. Song, M. Gielen, M. Kemmer, M. Biesemans, R. Willem, D. de Vos. *Appl. Organomet. Chem.*, **17**, 305 (2003).
[33] M. Nath, S. Pokharia, R. Yadav. *Coord. Chem. Rev.*, **215**, 99 (2001).
[34] A. Růžička, L. Dostál, R. Jambor, V. Buchta, J. Brus, I. Císařová, M. Holčapek, J. Holeček. *Appl. Organomet. Chem.*, **16**, 315 (2002).
[35] J.J. Zukerman. *Adv. Organomet. Chem.*, **9**, 21 (1970).
[36] A.G. Davies, P.J. Smith. *Comprehensive Organometallic Chemistry*, Vol. 2, p. 519, Pergamon Press, Oxford (1982).
[37] C. Silvestru, I. Haiduc, F. Caruso, M. Rossi, B. Mahieu, M.J. Gielen. *J. Organomet. Chem.*, **448**, 75 (1993).
[38] M.G. Clark, A.G. Maddock, R.H. Platt. *J. Chem. Soc., Dalton Trans.*, 281 (1972).
[39] T.K. Sham, G.M. Bancroft. *Inorg. Chem.*, **14**, 2281 (1975).
[40] T.P. Lockhart, W.F. Manders, E.O. Schlemper, J.J. Zuckerman. *J. Am. Chem. Soc.*, **108**, 4074 (1986).
[41] T.P. Lockhart, W.F. Manders, J.J. Zuckerman. *J. Am. Chem. Soc.*, **107**, 4546 (1985).
[42] T.P. Lockhart, W.F. Manders. *Inorg. Chem.*, **25**, 892 (1986).
[43] J. Holeček, M. Nadvornik, K. Handlir, A. Lyčka. *J. Organomet. Chem.*, **315**, 299 (1986).
[44] R. Colton, D. Dakternieks. *Inorg. Chim. Acta*, **148**, 31 (1988).
[45] ''Powder Diffraction File, Sets 1-10, Joint Committee on Powder Diffraction Standards,'' Philadelphia, PA, p. 213 (1967).
[46] H.P. Klug, L.E. Alexander. *X-ray Diffraction Procedures for Polycrystalline and Amorphous Materials*, 2nd Edn, Chapter 9, Wiley, New York (1974), .